Antagonism of Sphingosine-1-Phosphate Receptors by FTY720 Inhibits Angiogenesis and Tumor Vascularization

Kenneth LaMontagne,[1] Amanda Littlewood-Evans,[2] Christian Schnell,[2] Terence O'Reilly,[2] Lorenza Wyder,[2] Teresa Sanchez,[3] Beatrice Probst,[2] Jeannene Butler,[1] Alexander Wood,[4] Gene Liau,[4] Eric Billy,[2] Andreas Theuer,[2] Timothy Hla,[3] and Jeanette Wood[2]

[1]Novartis Institutes for BioMedical Research, East Hanover, New Jersey; [2]Novartis Institutes for BioMedical Research, Basel, Switzerland; [3]University of Connecticut Health Center, Farmington, Connecticut; and [4]Novartis Institutes for BioMedical Research, Inc., Cambridge, Massachusetts

Abstract

FTY720, a potent immunomodulator, becomes phosphorylated *in vivo* (FTY-P) and interacts with sphingosine-1-phosphate (S1P) receptors. Recent studies showed that FTY-P affects vascular endothelial growth factor (VEGF)–induced vascular permeability, an important aspect of angiogenesis. We show here that FTY720 has antiangiogenic activity, potently abrogating VEGF- and S1P-induced angiogenesis *in vivo* in growth factor implant and corneal models. FTY720 administration tended to inhibit primary and significantly inhibited metastatic tumor growth in a mouse model of melanoma growth. In combination with a VEGFR tyrosine kinase inhibitor PTK787/ZK222584, FTY720 showed some additional benefit. FTY720 markedly inhibited tumor-associated angiogenesis, and this was accompanied by decreased tumor cell proliferation and increased apoptosis. In transfected HEK293 cells, FTY-P internalized $S1P_1$ receptors, inhibited their recycling to the cell surface, and desensitized S1P receptor function. Both FTY720 and FTY-P apparently failed to impede VEGF-produced increases in mitogen-activated protein kinase activity in human umbilical vascular endothelial cells (HUVEC), and unlike its activity in causing S1PR internalization, FTY-P did not result in a decrease of surface VEGFR2 levels in HUVEC cells. Pretreatment with FTY720 or FTY-P prevented S1P-induced Ca^{2+} mobilization and migration in vascular endothelial cells. These data show that functional antagonism of vascular S1P receptors by FTY720 potently inhibits angiogenesis; therefore, this may provide a novel therapeutic approach for pathologic conditions with dysregulated angiogenesis. (Cancer Res 2006; 66(1): 221-31)

Introduction

Angiogenesis, the formation of new blood vessels from preexisting vessels, is a normal aspect of the physiologic remodeling processes that occurs in wound healing and during the female reproductive cycle. However, in pathologic situations, such as rheumatoid arthritis, diabetic retinopathy, and tumor development, abnormally enhanced neovascularization is a major contributory factor for disease progression (1, 2). The initiation of pathology-associated angiogenesis involves vascular permeability changes, driven by angiogenic factors, such as vascular endothelial growth factor (VEGF; ref. 3). This leads to fibrin deposition, plasmin activation, basement membrane degradation, and ultimately endothelial cell migration and proliferation, recruitment of mural cells, and vessel maturation (4).

Sphingosine-1-phosphate (S1P), a bioactive sphingolipid metabolite secreted by platelets upon activation, is a potent proangiogenic molecule, which acts by binding various members of the G-protein–coupled receptor (GPCR) family of S1P receptors (S1P-R; refs. 5, 6). A novel immunosuppressant agent currently in clinical trials for renal transplant rejection (FTY720) and its metabolite of cellular kinase(s) FTY720 phosphate (FTY-P; ref. 7) bear structural similarity to sphingosine and S1P, respectively. FTY-P binds at low nanomolar concentrations to four of five S1P-Rs, $S1P_1$, $S1P_3$, $S1P_4$, and $S1P_5$ (8). Recently, we have shown that FTY-P can act in a similar manner to S1P, stimulating endothelial cell signaling, migration, survival, and differentiation (9). By recruiting adherens junction proteins to the endothelial cell-cell junctions (10), FTY720 has also been shown to antagonize VEGF-induced permeability of blood vessels (10, 11). Tumor-associated blood vessels are permeable and elicit tissue extracellular fluid extravasation; therefore, this prompted us to investigate whether FTY720 exerts any antiangiogenic and antitumor activity *in vivo* by affecting vessel permeability.

In this report, we show that FTY720 at clinically relevant doses, inhibits both S1P- and VEGF-induced angiogenesis, and impedes primary and metastatic tumor growth in a murine model of melanoma. Additionally, combination of FTY720 with the VEGFR tyrosine kinase inhibitor PTK787/ZK222584 (PTK/ZK) further reduces the growth of the tumors and metastases. These findings suggest that targeting S1P receptors may provide a novel therapeutic approach in cancer treatment.

Materials and Methods

Materials. S1P was purchased from BioMol Research Labs, Inc. (Plymouth Meeting, PA). FTY720 and all other related compounds mentioned herein were generously provided by the Novartis Transplantation Group (Basel, Switzerland) and prepared as described previously (9). Human umbilical vein endothelial cells (HUVEC), from Vec Technologies, Inc. (Rensselaer, NY), were maintained in MCDB 131 Complete media (Vec Technologies) and were used from passages 4 to 7.

Female C57/Bl6 mice were obtained from The Jackson Laboratory (Bar Harbor, ME) or IFFA Credo (L'Arbresle, France). Female mice (MAG and NIH/Tif), weighing 18 to 20 g (6-8 weeks old), were obtained from the Novartis animal breeding facility. All animal experiments done in Switzerland were done in strict adherence to the Swiss law for animal protection,

Note: K. LaMontagne and A. Littlewood-Evans contributed equally to this work.

K. LaMontagne and J. Butler are currently at J&J PRD, Raritan, NJ (klamontagne@prdus.jnj.com).

PTK787/ZK222584 is a co-development compound by Novartis AG and Schering AG.

Requests for reprints: Amanda Littlewood-Evans, Novartis NIBR AG, K125.1.20, Klybeck Strasse, Basel, CH4002, Switzerland. Phone: 41-61-696-1023; Fax: 41-61-696-6242; E-mail: amanda.littlewood-evans@novartis.com.

doi:10.1158/0008-5472.CAN-05-2001

and experiments done in The United States were conducted in accordance with the Novartis Animal Care and Use Committee.

The S1P analogues FTY720, NVP-AAL149, and NVP-AAL151 and the VEGFR receptor tyrosine kinase inhibitor NVP-AAL993 were synthesized by Novartis AG (Basel, Switzerland). The VEGFR receptor tyrosine kinase inhibitor PTK/ZK was synthesized by Schering AG (Berlin, Germany) in collaboration with Novartis.

Fluorescence imaging plate reader Ca^{2+} mobilization assay. Fluorescence imaging plate reader (FLIPR) assay with HUVECs was carried out as described previously (9). Briefly, titrated compounds were preincubated with cells in a 96-well plate for 3 hours. Subsequently, the cell plates and ligand plates (containing 500 nmol/L S1P final concentration) were loaded into the FLIPR. The inhibition of S1P-induced calcium mobilization by FTY720, FTY-P, and NVP-AAL151 was plotted with EXCEL and SigmaPlot, and IC_{50} was determined for each compound.

Migration assay. The 4-hour migration assay was carried out using the BD Biocoat FluoroBlok System as described previously (9). HUVECs were preincubated for 30 minutes with compounds in MCDB 131 basal media (Vec Technologies), containing 0.1% bovine serum albumin (BSA, delipidized, BD Biosciences). S1P was diluted in the same media to a final concentration of 500 nmol/L and added to the bottoms of the assay plate wells. Migrated cells were stained with Calcein AM (Molecular Probes, Eugene, OR) and quantified with a CytoFluor II (PerSeptive Biosystems, Framingham, ME) fluorescent plate reader.

Mouse corneal micropocket assay. This method has been previously described in detail (12). Briefly, pellets containing the slow-release polymer Hydron and sucralfate with 180 ng $rHuVEGF_{165}$ were implanted into the cornea of female C57BL/6J mice. Daily oral treatment with FTY720 (0.3 or 3 mg/kg) or vehicle (10 mL/kg, 5% w/v glucose) was started 24 hours later. The eyes were routinely examined by slit-lamp biomicroscopy (Nikon FS-3V), and on day 6, mice were sacrificed, and the vascular response was quantified using a linear reticule through the slit lamp. Inhibition was determined by the formula $0.2\pi \times$ new blood vessel length $\times$ clock hours of neovessels. The circumferential zone was measured as clock hours with a 360-degree reticule (where 30 degrees of arc equals 1 clock hour). The data are reported as the % inhibition of blood vessel growth compared with the vehicle group.

Chamber assay (S1P and VEGF dependent). This assay has been described previously (13). Briefly, sterile porous Teflon chambers were filled with 0.8% agar (BBL Nr. 11849, Becton Dickinson, Meylan, France) containing heparin (20 units/mL) with or without growth factors: $VEGF_{165}$ (2 μg/mL; Tumor Center, Freiburg, Germany), or 5 μmol/L S1P (ANAWA Biomedical, Zürich, Switzerland). The chamber was implanted s.c. on the dorsal flank of female mice (MAG and NIH/Tif). Animals were treated with FTY720 (0.3 or 3 mg/kg orally), NVP-AAL151 or NVP-AAL149 (2.5 mg/kg i.v.) or NVP-AAL993 (100 mg/kg orally) 4 to 6 hours before chamber implantation and then once daily for a further 3 days. On the fourth day after implantation, animals were sacrificed, and the vascularized fibrous tissue formed around each implant carefully removed and weighed. Tissue samples were then homogenized in 1 mL of radioimmunoprecipitation assay (RIPA) buffer [50 mmol/L Tris-HCl (pH 7.2), 120 mmol/L NaCl, 1 mmol/L EDTA, 6 mmol/L EGTA, 1% (v/v) NP40, 20 mmol/L NaF, to which fresh 1 mmol/L phenylmethylsulfonyl fluoride and 1 mmol/L Na-vanadate were added], centrifuged, and filtered. The amount of hemoglobin present in the supernatant was determined by spectrophotometric analysis at 540 nm using the Drabkin reagent kit (Sigma hemoglobin #525, Sigma Chemical Co., Ltd., Poole, Dorset, England).

Tie-2 measurements. Tie-2 levels were determined using an ELISA method. Nunc (Naperville, IL) Maxsisorb 96-well plates were coated over night at 4°C with the capture antibody, anti-Tie-2 AB33 (UBI, Hauppauge, NY), with a concentration of 2 μg/mL (100 μL/well). Wells were washed in TPBS (Tween 80 PBS) and blocked by incubating with 3% Top-Block (Juro, Lucerne, Switzerland) for 2 hours at room temperature. After washing, 300 μg of protein lysates were incubated for 2 hours before further washing and addition of a complex of detection antibody, goat anti-mouse Tie-2 (R&D Systems, Minneapolis, MN; 0.5 μg/mL) and alkaline phosphate conjugated to monoclonal antibody (mAb) anti-goat (Sigma, St. Louis, MO; diluted 1:6,000) in TPBS + 0.1%Top-Block for 1 hour at room temperature. After washing, Tie-2 antibody complexes were detected by incubating with *p*-nitrophenyl phosphate (Sigma, tablets) and reading absorbance with an ELISA reader at 405 nm.

Recombinant human extracellular domain of Tie-2 fused to the constant regions of human IgG1 (sTie-2Fc) dissolved in RIPA buffer was used as standard in a concentration range from 0.1 to 300 ng/well (Tie-2Fc was a kind gift from Georg Martiny-Baron, Novartis).

VEGF-induced microvascular permeability. Heparin immobilized acrylic beads (50-100 μm in diameter) were incubated overnight with PBS/O or a solution of 1 μg VEGF in 10 μL PBS/O. Subsequently, the beads were implanted s.c. in both ears of female MAG mice (8-10 beads per ear). Vascular permeability of the newly formed vessels was visualized after 2 days using Evans blue dye (2%, 10 ml/kg) that was injected i.v. 5 minutes before sacrifice. Measurements of the dye extravasation area (mm^2) were carried out using pixel-based threshold in a computer-assisted image analysis software (KS-400 3.0 imaging system, Zeiss, Jena, Germany). Mice were treated with FTY720 (0.3 and 3 mg/kg orally) or PTK/ZK (100 mg/kg orally) 2 hours before Evans blue injection.

Tumor model. The syngeneic B16/BL6 murine melanoma model, previously shown to be responsive to antiangiogenic therapy (13), was used to evaluate the antitumor activity of FTY720. B16BL6 melanoma cells (kind gift from Dr. Isaiah J. Fidler, Texas Medical Center, Houston, TX) were cultured until confluency. Tumor cells (1 μL, 5×10^4/μL) was injected intradermally into the dorsal pinna of both ears of syngeneic female C57BL/6 mice. Measurements of primary tumor area (mm^2) were carried out on days 7, 14, and 21 after tumor cell inoculation using computer-assisted image analysis software (KS-400 3.0 imaging system, Zeiss) and a specially designed macro. From days 7 to 21, mice were treated orally once daily with either vehicle PEG300 (5 mL/kg), FTY720 (3 mg/kg), PTK/ZK (100 mg/kg), or a combination of the two compounds at the above doses. Mice were sacrificed on day 21, and cranial lymph node metastases were weighed and then frozen in ornithine carbamyl transferase cryofreezing medium for histologic analysis.

Histologic analysis and lectin perfusion. Lectin (200 μL) from *Ricinus communis* agglutinin-1, FITC conjugated (Vector Labs, Burlingame, CA), at a concentration of 1 μg/μL in sterile 0.9% NaCl was injected into the tail vein of a B16/BL6 melanoma bearing C57/B6J mouse. The mouse was left for 30 minutes before sacrifice and tumor excision. Frozen sections (12 μm) were subjected to immunohistochemical analysis as described previously (14). Antibodies used were rat anti-mouse CD31 (BD PharMingen, San Diego, CA; diluted 1:600 in PBS), rabbit anti-mouse active caspase 3 (Oncogene, Uniondale, NY; diluted 1:10 in PBS), and rabbit anti mouse Ki67 (Neomarkers, Fremont, CA; diluted 1:200 in PBS). Secondary antibodies were goat anti-rabbit or goat anti-rat ALEXA 568 or 488 (Molecular Probes, 1:400).

Fluorescence-activated cell sorting analysis. Mice bearing B16/BL6 melanoma tumors were treated daily for 7 days (days 7-14) with FTY720 (3 mg/kg orally), PTK/ZK (100 mg/kg orally) or the combination of both drugs. At the end of treatment, mice were sacrificed, cranial lymph node metastases were surgically removed and minced into small pieces, and a single-cell suspension was formed by collagenase/dispase treatment and subjected to fluorescence-activated cell sorting (FACS) analysis. Due to their small size, tumor cells were detected as a distinct population in the scatter plot and can be accordingly gated and enumerated.

HUVEC cells were treated with vehicle alone or FTY-P (10 and 100 nmol/L) for 30 minutes and were analyzed by FACS for VEGFR2 levels on the cell surface. Cells were trypsinized, washed twice with PBS containing 10% (v/v) fetal bovine serum (FBS), and incubated 10 minutes on ice before the addition of mouse mAb anti-VEGFR2/KDR 1495.12.14 (13) antibody developed within our laboratories in Novartis (2 μg mAb/10^6 cells). After 1 hour of incubation on ice, cells were washed twice in PBS plus 10% FBS, and RPE-labeled anti-mouse was added to the cells (BD PharMingen). FACS acquisition and analysis were done on a FACSCalibur using Cell Quest Software (Becton Dickinson).

Analysis of $S1P_1$ receptor localization. HEK293 cells expressing $S1P_1$-GFP fusion protein (15) were used in this assay. Cells were serum starved for 2 hours and treated with indicated concentrations of S1P or FTYP or

structural analogues as described (10). At specific times, cells were fixed and imaged on a Zeiss 510 confocal microscope as previously described (15).

Blood cell counts. Blood analysis was done using a commercially available blood analyzer ABC VET 16 (Axon Lab AG, Baden-Dättwil, Switzerland). Blood was collected in EDTA tubes via the vena cava inferior immediately after sacrifice of the mice by CO_2 inhalation. An aliquot (12 μL) of EDTA-blood obtained from all groups of mice treated for 21 days was taken 24 hours after the last dose and analyzed for WBC, RBC, platelets, lymphocytes, monocytes, and granulocytes.

Proliferation assay. Subconfluent B16/BL6 melanoma cells were seeded at a density of 3×10^3 per well into 96-well plates and incubated at 37°C and 5% CO_2 in growth medium (10% FBS in MEM EBS, Amimed). After another 24 hours, the medium was renewed and PTK787/ZK222584, FTY720, FTY-P, or vehicle were added. After 8 hours of incubation, bromodeoxyuridine (BrdUrd) labeling solution was added, and cells were incubated a further 16 hours before fixation, blocking, and addition of peroxidase-labeled anti-BrdUrd antibody. Bound antibody was then detected using 3,3′ 5,5′-tetramethylbenzidine substrate, which forms a colored reaction product that is quantified spectrophotometrically at 450 nm.

Apoptosis assay. Subconfluent B16/BL6 melanoma cells were seeded at a density of 3×10^3 per well into 96-well plates and incubated at 37°C and 5% CO_2 in growth medium (10% FCS in MEM EBS, Amimed). After another 24 hours, the medium was renewed and PTK787/ZK222584, FTY720, FTY-P, or vehicle was added. Twenty-four hours later, induced cell death was measured photometrically through determination of cytoplasmic histone-associated DNA fragments, upon instructions of the supplier from the kit (Cell Death Detection ELISA^{PLUS}, Roche, Indianapolis, IN).

Western analysis. HUVECs at 80% confluency in EBM medium containing 0.5% (v/v) FBS were incubated with 500 nmol/L of either FTY720, FTY-P, or PTK/ZK for either 20 minutes or 1 hour. For the last 10 minutes of the incubation time, some of the HUVECs were stimulated with VEGF 10 ng/mL, and cells were subsequently lysed with RIPA buffer [50 mmol/L Tris-HCl (pH 7.2), 120 mmol/L NaCl, 1 mmol/L EDTA (pH 8), 6 mmol/L EGTA (pH 8.5), 1% (v/v) NP40, and 20 mmol/L NaF]. Ten micrograms of lysates were run on a 10% SDS gel and blotted. The gel was first probed with p44/42 mitogen-activated protein kinase (MAPK) antibody (Cell Signaling, Beverly, MA) and then stripped and reprobed with an α-tubulin antibody (Neomarkers) to control for equal loading.

Statistical analyses. Results are presented as mean ± one SE. Between-group differences used one-way ANOVA or two-way ANOVA employing Holm-Sidak tests for post hoc comparisons (either pairwise or versus controls). In some cases, the data were normalized by taking log10 before statistical analyses. For all tests, the level of significance was set at $P < 0.05$. Statistical calculations were done using SigmaStat 3.1 (Jandel Scientific, San Rafael, CA).

Results

FTY720 inhibits S1P-driven angiogenesis. Because S1P is a proangiogenic factor, we tested the effects of the S1PR modulator FTY720 (and analogues) in an S1P-driven angiogenesis agar chamber model (see Fig. 1*A* and *C*). We carried out the experiment in the same manner as the VEGF-driven chamber model previously used to characterize the VEGFR inhibitor PTK787/ZK222584 (PTK/ZK; ref. 13) but substituting S1P for VEGF. The effects of FTY720 at 3 and 0.3 mg/kg, an analogue NVP-AAL151 and its inactive enantiomer NVP-AAL149 both at 2.5 mg/kg, and a VEGF receptor tyrosine kinase inhibitor NVP-AAL993 at 100 mg/kg were assessed. The mice received a single administration of vehicle or compound 4 to 6 hours before implantation and were subsequently treated once daily for 3 days before explanting the chamber. In this time, a new blood vessel–rich tissue is formed around the implanted chamber. This tissue was removed, weighed, and analyzed for total amount of hemoglobin (a measure for vascularity and hemorrhage) and Tie-2 protein (indicative of endothelial cell amount and therefore vascularity only) in the tissue.

S1P was overall a weaker promoter of the indices of angiogenesis in this chamber model compared with VEGF (Fig. 1). FTY720 at doses of 0.3 and 3 mg/kg reduced the weight of newly formed tissue and its hemoglobin and blood vessel content in the S1P-driven agar implant model (Fig. 1*A*). NVP-AAL151 also functioned as an inhibitor in this model, whereas NVP-AAL149 was considerably weaker. As expected, the VEGFR tyrosine kinase inhibitor NVP-AAL993 did not exert any influence on the S1P-driven angiogenesis model (Fig. 1*C*). These results show that FTY720 and NVP-AAL151 are able to inhibit S1P-driven angiogenesis *in vivo*.

FTY720 inhibits VEGF-driven angiogenesis. We further tested if FTY720 and its analogues at the same doses as above were able to inhibit VEGF-driven angiogenesis using the s.c. implant model (Fig. 1*B* and *C*). VEGF-filled agar chambers (Fig. 1*B, gray columns*) produced increased weight as well as amount of hemoglobin and Tie-2 in the newly formed tissue compared with an agar implant with no growth factor (Fig. 1*B, black columns*). FTY720 at 3 and 0.3 mg/kg inhibited the VEGF-dependent increased weight ($P < 0.001$ versus VEGF control) and Tie-2 ($P < 0.001$ versus VEGF control) and hemoglobin ($P < 0.05$ versus VEGF control) content of the tissue. There was a tendency for the 3 mg/kg dose to be more active than the 0.3 mg/kg dose in all of the variables evaluated. However, this only reached statistical significance with hemoglobin content. The immunosuppressive properties of FTY720 were evident by the reduced number of WBC, specifically lymphocytes, circulating in the blood (data not shown). Platelets, granulocytes, and RBC were unaffected (data not shown).

With the exception of NVP-AAL149 (the inactive enantiomer that is not phosphorylated by sphingosine kinase; see refs. 9, 10), all compounds were able to inhibit the increase in weight of the newly formed tissue, hemoglobin, and Tie-2 content in this model (Fig. 1*C*). NVP-AAL149 was significantly less active than either NVP-AAL151 or NVP-AAL993 in terms of impairing tissue accumulation and Tie-2 levels ($P < 0.001$), hemoglobin content of the tissue (versus NVP-AAL151, $P = 0.013$; versus NVP-AAL993, $P = 0.005$). Interestingly, in this VEGF-driven angiogenesis model, the VEGFR inhibitor NVP-AAL993 and the S1PR signaling modulator NVP-AAL151 were not statistically different in their inhibitory effects (mg tissue, $P = 0.9$; hemoglobin levels, $P = 0.3$; Tie-2 levels, $P = 0.5$). These results show that at doses producing leukopenia, FTY720 and its analogues have potent antiangiogenic activity in a well-established *in vivo* angiogenesis model driven by two distinct proangiogenic factors.

We also tested the ability of FTY720 to block neoangiogenesis in the mouse corneal pocket assay, a widely used angiogenesis model. In this model (12), VEGF pellets were surgically implanted into avascular corneas of C57BL/6 mice to induce a robust angiogenesis response (Fig. 1*D*). Twenty-four hours after implantation, mice were treated with either vehicle alone or FTY720 at 0.3 or 3 mg/kg orally once per day. The eyes were examined on postoperative days 3 through 6, and the induced vascular response was measured. Oral treatment with FTY720 caused a marked (versus controls: 0.3 mg/kg FTY720, $P = 0.002$; 3 mg/kg FTY720, $P < 0.001$) and apparently dose-dependent inhibition of new blood vessel formation (3 mg/kg FTY720 superior to 0.3 mg/kg, $P = 0.02$).

FTY720 reduces leakiness of blood vessels. Because blockade of the hemoglobin response in the chamber model may reflect an effect on vascular permeability rather than an effect on new vessel

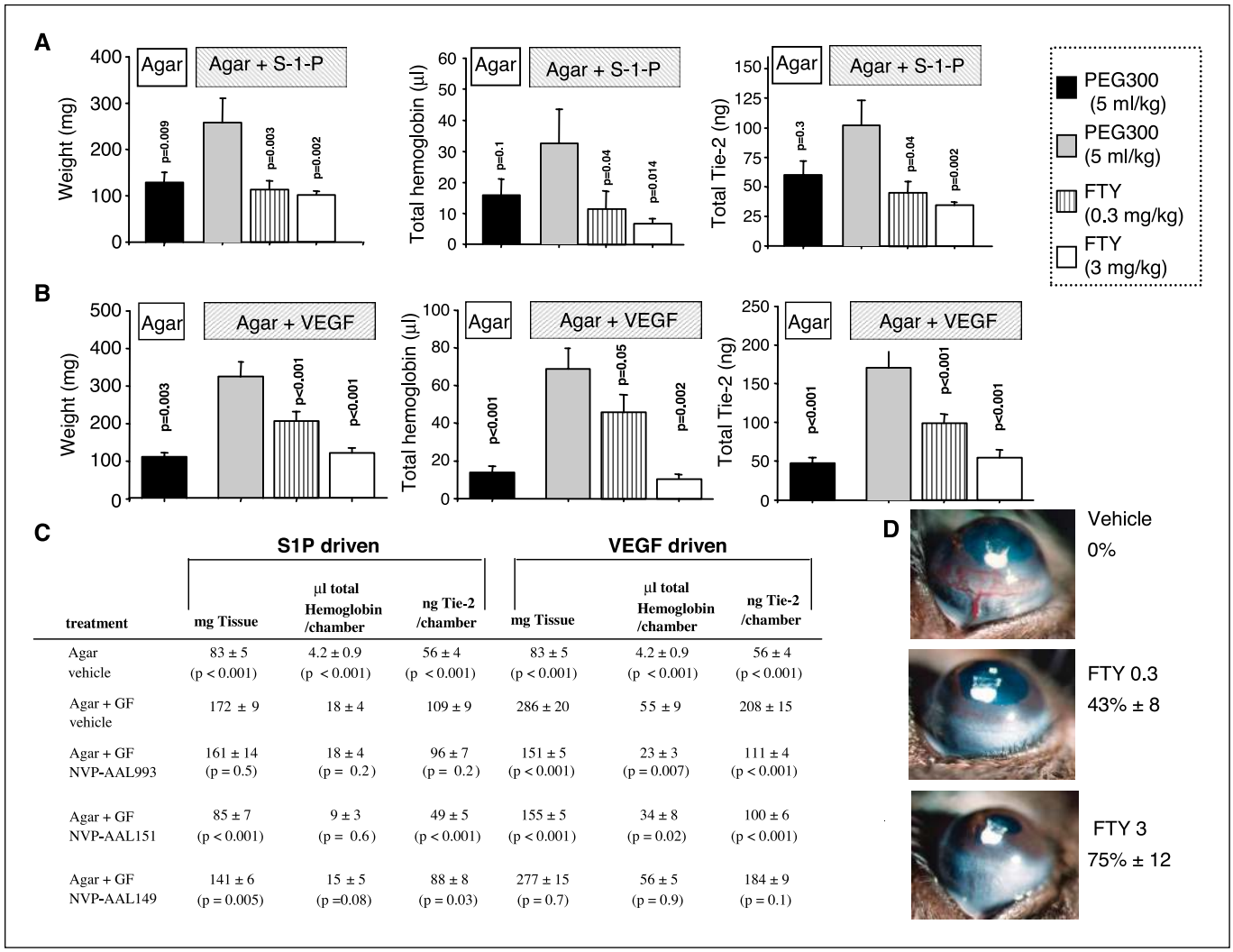

treatment	S1P driven: mg Tissue	S1P driven: µl total Hemoglobin /chamber	S1P driven: ng Tie-2 /chamber	VEGF driven: mg Tissue	VEGF driven: µl total Hemoglobin /chamber	VEGF driven: ng Tie-2 /chamber
Agar vehicle	83 ± 5 (p < 0.001)	4.2 ± 0.9 (p < 0.001)	56 ± 4 (p < 0.001)	83 ± 5 (p < 0.001)	4.2 ± 0.9 (p < 0.001)	56 ± 4 (p < 0.001)
Agar + GF vehicle	172 ± 9	18 ± 4	109 ± 9	286 ± 20	55 ± 9	208 ± 15
Agar + GF NVP-AAL993	161 ± 14 (p = 0.5)	18 ± 4 (p = 0.2)	96 ± 7 (p = 0.2)	151 ± 5 (p < 0.001)	23 ± 3 (p = 0.007)	111 ± 4 (p < 0.001)
Agar + GF NVP-AAL151	85 ± 7 (p < 0.001)	9 ± 3 (p = 0.6)	49 ± 5 (p < 0.001)	155 ± 5 (p < 0.001)	34 ± 8 (p = 0.02)	100 ± 6 (p < 0.001)
Agar + GF NVP-AAL149	141 ± 6 (p = 0.005)	15 ± 5 (p =0.08)	88 ± 8 (p = 0.03)	277 ± 15 (p = 0.7)	56 ± 5 (p = 0.9)	184 ± 9 (p = 0.1)

Figure 1. Antiangiogenic effect of FTY720. *A,* effect of FTY720 (0.3 or 3 mg/kg orally) or vehicle (PEG300, 100% 5 mL/kg orally) on an S1P-driven chamber model (5 µmol/L). Weight (*left*), total hemoglobin (*middle*), and Tie-2 levels (*right*) of the tissue are plotted. From two independent experiments were pooled (10-12 mice). *Columns,* mean; *bars,* SE. The statistical significance of inhibition compared with vehicle-treated S1P containing chambers was determined using one-way ANOVA with post hoc Holm-Sidak tests. *B,* effect of FTY720 (0.3 or 3 mg/kg orally) or vehicle (PEG300, 100% 5 mL/kg orally) on the VEGF-driven chamber model (2 µg/mL). Weight (*left*), total hemoglobin (*middle*), and Tie-2 levels (*right*) of the tissue are plotted. From two independent experiments were pooled (10-12 mice). *Columns,* mean; *bars,* SE. Statistical significance of inhibition was determined using one-way ANOVA with post hoc Holm-Sidak tests. *C,* treatment of mice with NVP-AAL993 (100 mg/kg orally), NVP-AAL149 (2.5 mg/kg i.v.), NVP-AAL151 (2.5 mg/kg i.v.), or vehicle (PEG300, 100% 5 mL/kg orally) in an S1P-driven (5 µmol/L) or VEGF-driven (2 µg/mL) agar chamber model (see *top*). The animals were sacrificed for measurement of the vascularized chamber-adherent tissues (weight and hemoglobin and Tie-2 content) 24 hours after the last dose (n = 10-12 per group, pooled data from two independent experiments per dose). *GF,* growth factor. Statistical significance of inhibition was determined using one-way ANOVA with post hoc Holm-Sidak tests. *D,* C57/BL6J mouse corneal pocket assay. Photomicrographs showing vascularization induced by VEGF-implanted pellets after 6 days of treatment with vehicle (5% glucose in water), 0.3 mg/kg FTY720, or 3 mg/kg FTY720. *Numbers,* % inhibition of blood vessel growth (mean ± SE). Both the high-dose FTY720 group (P < 0.001) and the low-dose group (P = 0.002) were statistically significantly different from controls (one-way ANOVA with post hoc Holm-Sidak test). The experiment was done two separate times. Representative experiment. Quantitative data pooled from both experiments (n = 6 per group).

formation, we investigated the effect of FTY720 in a specific assay for vascular permeability (Fig. 2). For this purpose, VEGF-soaked beads were implanted s.c. into one ear of a mouse, which produces new but leaky and torturous vessel formation over a period of 2 days. The other ear of the same mouse is implanted with PBS soaked beads as a control. After 2 days, Evans blue is injected i.v., and images of the ears are taken. Blood vessel leakiness is assessed initially by visual inspection (Fig. 2*A*) and by image analysis determination of the area of extravasated Evans blue dye (Fig. 2*A* and *B*). Vehicle, PTK/ZK (100 mg/kg), or 0.3 or 3 mg/kg FTY720 were administered 2 hours before Evans blue injection. Two-way ANOVA indicated that VEGF increased vessel leakiness compared with that produced by control beads (P < 0.001), and both compounds alone inhibited both basal and VEGF-induced vascular permeability changes. At both 0.3 and 3 mg/kg, FTY720 inhibited basal leakiness (likely to be caused by wounding during implantation or inflammatory processes associated with the intracorporal presence of a foreign body; Fig. 2*A* and *B*) as well as VEGF-induced leakiness of the vessels. As expected, the two VEGF receptor tyrosine kinase inhibitors NVP-AAL993 (not shown) and PTK/ZK also effectively reduced leakiness of the vasculature in this model (Fig. 2). When comparing (two-way ANOVA) the effect of treatment in the absence of VEGF stimulus, PTK/ZK or FTY720 at 0.3 or 3 mg/kg inhibited vascular leakiness, but these treatments

were not significantly different from each other (all *P*s < 0.05). The presence of VEGF clearly promoted vascular permeability. Within the VEGF-treated groups, PTK/ZK and 0.3 mg/kg FTY720 impaired vascular permeability by (P = 0.022 and P < 0.001 versus controls), and 3 mg/kg FTY720 produced an effect greater than either of the other two active treatments (Fig. 2*B*). These results indicate that part of the observed pharmacologic antiangiogenic activity of FTY720 may be due to abrogation of the increases in vascular permeability caused by VEGF.

FTY720 pretreatment inhibits S1P-stimulated migration and calcium mobilization *in vitro*. Because FTY720 was recently shown to act as a functional antagonist on $S1P_1$ receptors on T cells, inhibiting their egress from lymph nodes (16), we assessed whether FTY720 can also modulate the response of endothelial cells to S1P. We first examined the effect of FTY720, FTY-P, NVP-AAL151, and NVP-AAL149 on S1P-driven endothelial migration *in vitro* (data not shown). Compounds were preincubated with HUVEC for 30 minutes before the cells were allowed to migrate towards S1P (500 nmol/L) in the continuing presence of compounds. FTY720, FTY-P, and NVP-AAL151 were all able to significantly inhibit S1P-induced HUVEC migration with IC_{50} values of 6.5, 2.5, and 7.4 nmol/L, respectively, whereas NVP-AAL149 was inactive at all doses tested (>250 nmol/L). Because the prodrug FTY720 was active in this assay, this suggested that the 4-hour incubation time of the assay was sufficient for conversion of FTY720 to FTY-P by sphingosine kinase and for the latter form to subsequently inhibit the S1P-mediated migration of cells (17).

Activation of S1PR by S1P causes G-protein–coupled activation and mobilization of calcium from the endoplasmic reticulum (9, 18). We tested FTY720 and its analogues in this assay to see if they could antagonize S1P-induced Ca^{2+} mobilization (data not shown). The compounds were preincubated with HUVEC for 3 hours before the assay to allow the prodrugs to be phosphorylated by sphingosine kinase. FTY-P, FTY720, and NVP-AAL151 were all able to block the S1P-driven calcium mobilization with IC_{50} values of 55, 164, and 156 nmol/L, respectively, whereas NVP-AAL149 was unable to inhibit the S1P response (>34.4 μmol/L). The IC_{50} differences observed between the migration assay and Ca^{2+} mobilization are probably due to the longer incubation period (FTY720 converting to FTY-P) in the migration assay as well as the difficulty of inhibiting the amplification of signaling in the Ca^{2+} mobilization assay.

FTY-P internalizes $S1P_1$. To investigate the mechanism by which FTY720 and its analogues are modulating the S1P-driven responses, we incubated HEK293 cells stably expressing an $S1P_1$-GFP fusion protein (15) with 10 nmol/L of either S1P or FTY-P for 60 minutes and analyzed the localization of $S1P_1$ by confocal fluorescence imaging. $S1P_1$-GFP is normally expressed on the cell surface (Fig. 3*A*). Addition of S1P at 10 nmol/L did not affect the localization of this receptor; however, addition of FTY-P at the same concentration resulted in the internalization of $S1P_1$ as detected by the punctated endosomal appearance for $S1P_1$. An additional experiment was designed to investigate recycling of the receptor back to the surface of HEK293 cells (Fig. 3*B*). In this case, 100 nmol/L of S1P or FTY-P were added to the cells. This high dose of ligand resulted in receptor internalization in both cases after 60 minutes, although a significantly greater internalization was observed with the FTY-P treatment. The ligands were subsequently washed out, and the cells were allowed to recover for 60 minutes.

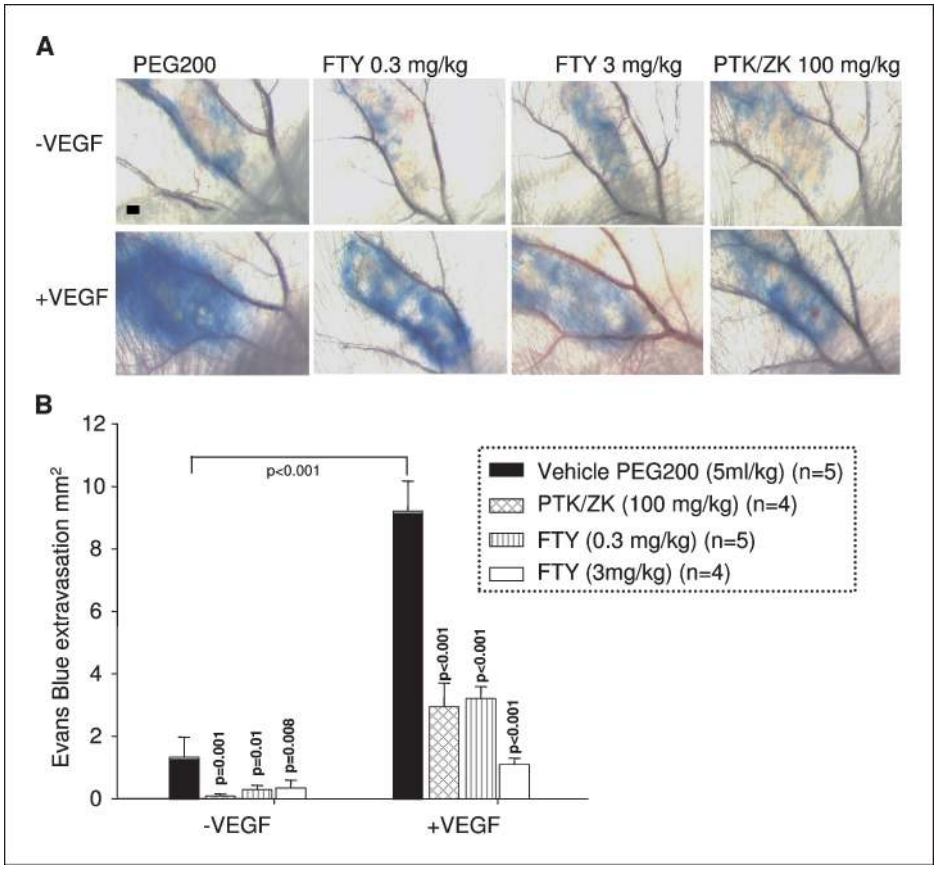

Figure 2. FTY720 reduces leakiness of vessels. *A,* photomicrographs showing leakage of Evans blue from vessels with implanted PBS-soaked beads (*top*) and VEGF-soaked beads (*bottom*). Treatment with FTY720, PTK/ZK, or vehicle. Bar, 1 mm. This experiment was done twice. Representative experiment. *B,* measurements of the dye extravasation area (mm^2) were carried out using computer-assisted image analysis software. *Columns,* mean; *bars,* SE. *P*s are from one-way ANOVA with post hoc Holm-Sidak tests.

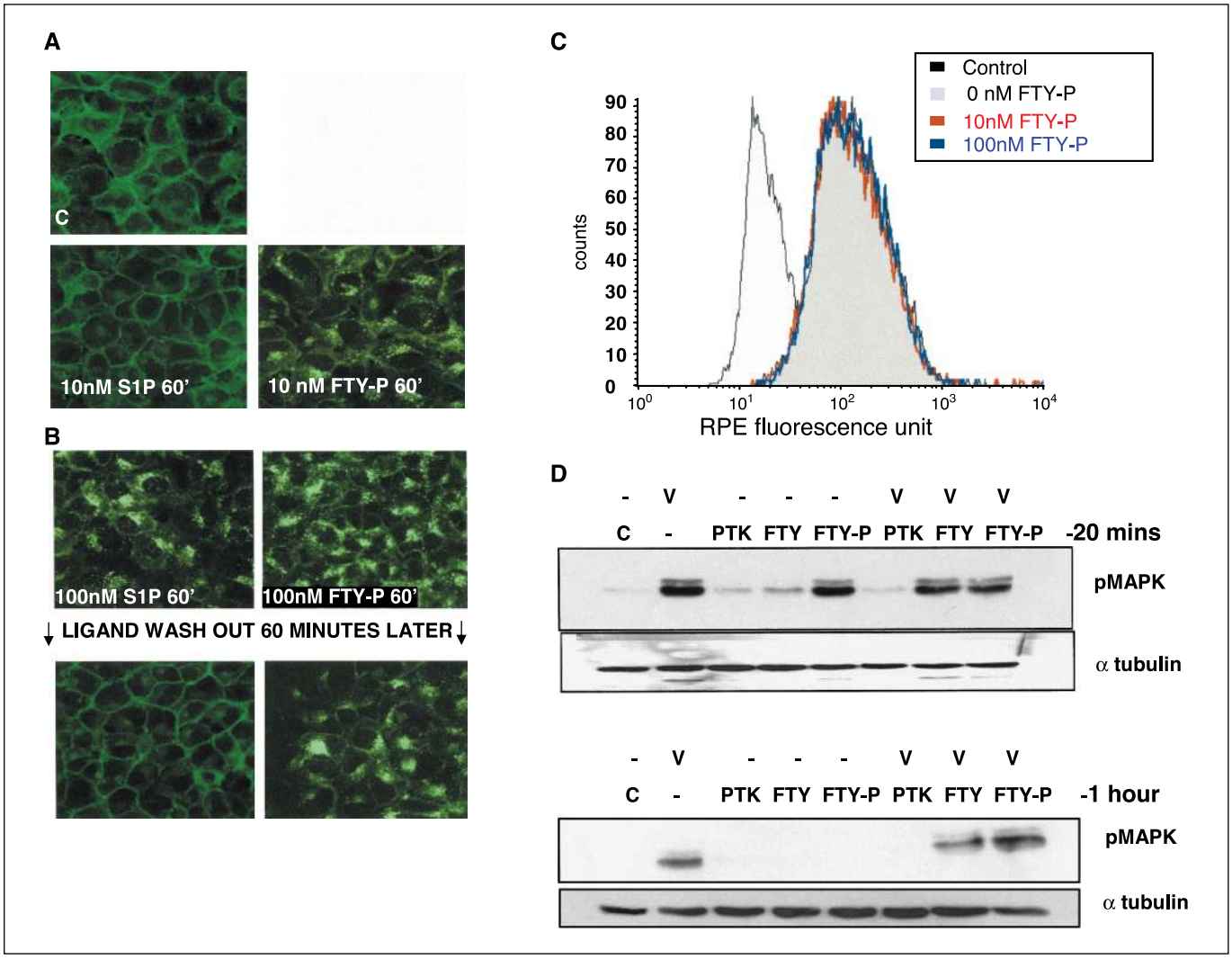

Figure 3. FTY-P internalizes $S1P_1$, does not affect VEGFR levels at the endothelial cell surface, and does not affect VEGF induced pMAPK. *A,* HEK293 cells transfected with $S1P_1$-GFP were incubated with 10 nmol/L of either S1P or FTY-P, or vehicle (*C*) for 60 minutes before imaging for $S1P_1$-GFP in a confocal microscope. *B,* HEK293 cells transfected with $S1P_1$-GFP were cultured together with 100 nmol/L of either S1P or FTY-P for 1 hour. Some representative wells were imaged. The remaining wells were washed briefly and incubated with medium minus the ligands for a further hour before imaging. *C,* FTY-P treatment does not lead to VEGFR2 internalization. HUVECs were analyzed for cell surface VEGFR2 levels by FACS analysis following 30 minutes of incubation with FTY-P or vehicle. Control (omission of primary antibody) and FTY-P at 0, 10, and 100 nmol/L. Positive cell surface staining for VEGFR2 (*gray area*). Effect of incubation for 30 minutes with FTY-P at 10 nmol/L (*red*) and 100 nmol/L (*blue*) on VEGFR2 surface level. *Black line,* antibody control. *D,* pMAPK Western blot analysis in HUVECs; 500 nmol/L of FTY720 (*FTY*), FTY-P, or PTK/ZK were incubated for 20 minutes (*top two blots*) or for 1 hour (*bottom two blots*) with HUVECs. For the last 10 minutes, cells were either stimulated with 10 ng/mL VEGF (*v*) or were vehicle controls (−). Western blots were first probed with pMAPK antibody and then were stripped and reprobed for equal loading with the housekeeping gene *α-tubulin*.

The receptor was recycled back to the surface only when the cells had been pretreated with S1P. In contrast, the $S1P_1$ receptor of the FTY-P treated cells remained protractedly internalized.

This irreversible internalization of $S1P_1$ associated with impaired S1P signaling thus renders the cells less responsive to S1P and may explain how FTY720, when converted to FTY-P by preincubation, is inhibiting the S1P-induced responses.

Analysis of VEGFR2 at the endothelial cell surface upon treatment with FTY-P. We next investigated the effect of the compound on cell surface VEGFR2 levels because we have shown that FTY720 also inhibits VEGF-induced angiogenesis. Either when incubated for 30 minutes with HUVECs before FACS analysis (Fig. 3*C*), or 30 minutes of incubation followed by a wash out of compound for 2 hours (data not shown), FTY-P did not affect the levels of VEGFR2 at the endothelial cell surface. This strongly suggests that FTY-P fails to modulate VEGF-induced angiogenesis by internalizing or reducing the levels of cell surface VEGFR2.

Phospho-MAPK stimulation in HUVECs. To investigate whether FTY720 or FTY-P was inhibiting VEGF-induced signaling, we looked at basal and VEGF-stimulated phospho-MAPK (pMAPK) in HUVECs. pMAPK is a downstream signaling component in both the VEGF and S1P signaling pathway (19, 20). We incubated FTY720, FTY-P, and PTK/ZK each at 500 nmol/L for either 20 minutes or for 1 hour and looked at pMAPK levels by Western blot (Fig. 3*D*). After 20 minutes, FTY-P and VEGF were both able to stimulate pMAPK, whereas FTY720 was not, due to the fact that this compound needs to be phosphorylated to activate S1PR signaling. The VEGF-induced phosphorylation was blocked by the VEGFR tyrosine kinase inhibitor PTK/ZK but was not blocked by

either FTY720 or FTY-P. After a 1-hour incubation with the compounds, FTY-P was no longer able to elicit a pMAPK signal, likely due to the S1P receptor internalization as described above. As seen in the shorter incubation experiment, both FTY720 and FTY-P had no effect on VEGF-induced pMAPK.

FTY720 inhibits melanoma growth in an orthotopic syngeneic mouse model. FTY720 was then evaluated as an antitumor and antimetastasis agent in a syngeneic orthotopic B16 melanoma model to determine whether it could affect tumor vascularization and thereby have an effect on tumor growth. The B16/BL6 melanoma cells are a subline derived from B16 cells and have a much more aggressive metastatic capability than their parental line (21). When B16/BL6 cells are implanted intradermally in the ear of a C57Bl6 mouse, a primary tumor forms (Fig. 4*A*) and subsequently cranial lymph node metastases develop (Fig. 4*B*). The metastases grow very rapidly, and new blood vessel formation is very evident for the following 1.5 weeks. The metastases become necrotic at later stages; therefore, we have found that the optimal time for antitumor therapy in this particular model is from 7 to 21 days. We used PTK/ZK, an angiogenesis inhibitor already shown to inhibit tumor growth in this model (13), as both a reference compound and combination partner for FTY720 to see whether we could obtain any additive effects by simultaneously blocking both VEGF and S1P receptor signaling.

After melanoma cell implantation, primary tumors were allowed to grow for 7 days before the start of a 14-day chronic regimen of either PTK/ZK (100 mg/kg) or FTY720 (3 mg/kg) or a combination of the two compounds (all administered orally, once per day). Mice were sacrificed on day 21, and primary tumors and lymph node metastases were analyzed. Primary tumor growth was inhibited with PTK/ZK by 54% ($P = 0.017$ versus controls) or FTY720 by 45%, although this level of inhibition was not statistically significant ($P = 0.079$ versus controls). Combination of the two compounds did not result in any additive effects compared with the single agents on the size of the primary tumor ($P = 0.025$ versus controls but $P > 0.05$ versus the other groups; Fig. 4*A*).

The VEGFR tyrosine kinase inhibitor PTK/ZK ($P = 0.013$), the immunomodulator FTY720 ($P = 0.03$), and the combination ($P = 0.002$) significantly reduced the metastasis weights (Fig. 4*B*). Although tending to be more active, the inhibitory activity of the combination was not statistically different than the monotherapies (combination versus PTK/ZK alone, $P = 0.17$ versus FTY720 alone, $P = 0.10$). Both PTK/ZK and FTY720, alone or in combination, were well tolerated at the administered doses, producing neither body

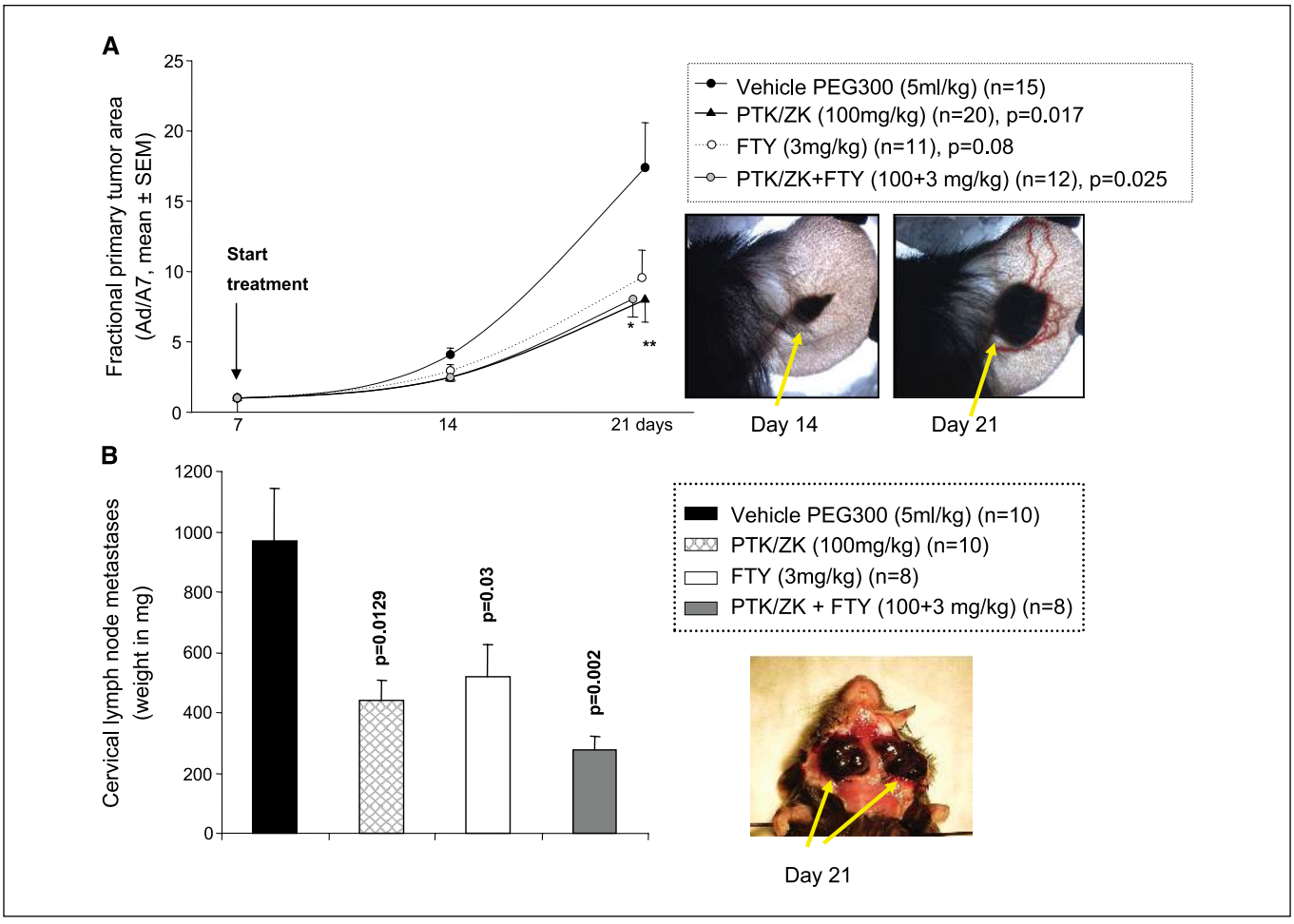

Figure 4. Effect of FTY720, PTK/ZK, and a combination on lymph node melanoma metastases in a syngeneic orthotopic mouse model. *A,* primary tumor growth measured at days 7, 14, and 21. Photomicrographs of a primary tumor (vehicle treated) growing in the ear of a mouse at days 14 and 21 (*arrows*). *B,* average weight of cervical lymph node metastasis after treatment. Photomicrograph of the spontaneously formed lymph node metastases in a vehicle-treated mouse after 21 days growth (*arrows*). *Columns,* mean; *bars,* SE. Pooled from two independent experiments. *P*s are from one-way ANOVA with post hoc Holm-Sidak tests.

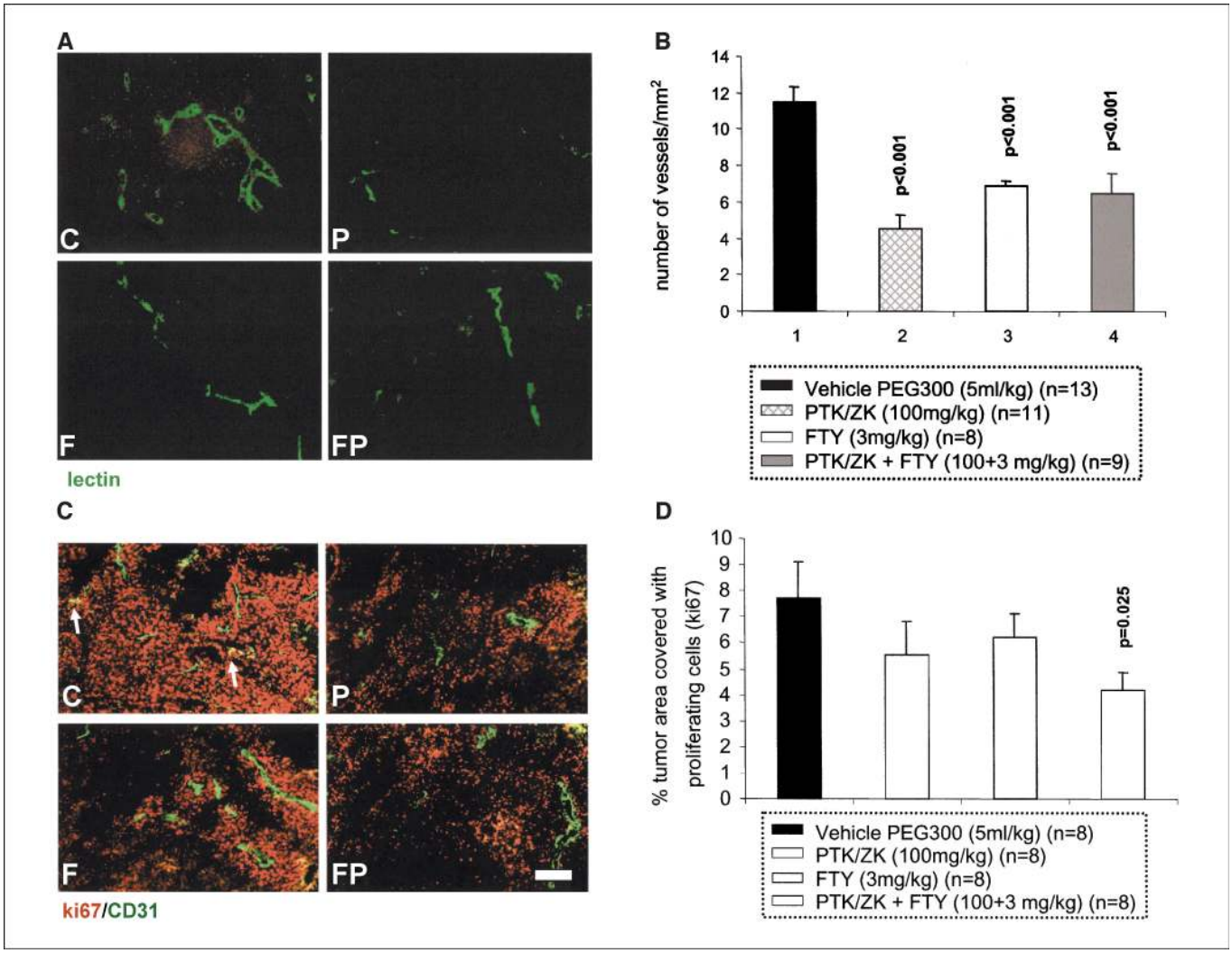

Figure 5. Vessel quantification in the B16/BL6 metastases and analysis of proliferation. *A,* photomicrographs of lectin perfusable vessels (*green*) in typical sections from lymph node metastases treated with vehicle (*C*), PTK/ZK (*P*), FTY720 (*F*), and a combination of the two compounds (*FP*). *B,* vessel density determined by counting lectin-positive vessels per mm^2 in a midsection of a lymph node metastasis. *Columns,* mean; *bars,* SE. Pooled from two independent experiments. *P*s are from one-way ANOVA with post hoc Holm-Sidak tests. *C,* photomicrographs showing typical immunohistochemically stained sections for vehicle (*C*), PTK/ZK (*P*), FTY720 (*F*), and a combination of the two drugs (*FP*). Ki67, a proliferation marker (*red*) and CD31 (*green*) highlights the vessels. *Arrows,* proliferating vessels (vehicle treated, *yellow*). Bar, 100 μm. *D,* quantification of area of tumor covered by Ki67-positive proliferating cells (*red cells*). Six representative fields per tumor section were photographed and quantified. *P*s are from one-way ANOVA with post hoc Holm-Sidak tests.

weight losses nor overt clinical signs indicative of tolerability problems.

To evaluate the effect of the compounds on tumor angiogenesis, the vasculature was perfused with lectin shortly before sacrifice of the animal, and vessel density in the metastases was quantified by image analysis (Fig. 5*A* and *B*). PTK/ZK and FTY720 alone both reduced functional blood vessel density significantly (both compounds alone $P < 0.001$ versus control). In addition, the combination of both compounds resulted in a robust reduction of vessel number, which also translated into a statistically significant reduction in vessel density ($P < 0.001$ versus control; Fig. 5*B*). The vessel density reduction observed with the combination treatment and monotherapies was not statistically significant between any of the groups.

Cell proliferation in the metastases was assessed by immunohistochemistry with a Ki67 antibody in combination with CD31 to highlight the vessels (Fig. 5*C*). Generally, healthy proliferating tumor cells were in close proximity to the blood vessels. The cells in the vessels themselves were also seen to be proliferating, especially in the vehicle-treated tumors (Fig. 5*C, arrows*). A combination of the two compounds resulted in a statistically significant reduction of tumor area covered with proliferating cells, when the staining was quantified by an image analyzer (Fig. 5*D*). We observed an ~2-fold reduction in Ki67-positive cells, when the combination was used to treat the mice that were not seen with the single agents.

We next did FACS analysis of the disaggregated tumor to investigate the viability of the tumor cells. The viable tumor cells themselves were easily identifiable by their small size, as they localized to a particular region on the FACS scatter plot (Fig. 6*A*, *gate R3*). The percentage of viable cells within the tumor was then assessed (Fig. 6*A*). Both compounds alone tended to result in reduction of viable melanoma cells (note that each of the monotherapy groups possessed a likely outlying data point), whereas the combination of

both drugs resulted in statistically significantly fewer viable tumor cells.

Further experiments sought to determine the levels of active caspase-3 in the tumors using histologic staining to determine whether cell death was occurring via apoptosis. CD31 staining was used to highlight the vasculature (Fig. 6*B*). Tumor cells that were distant from the vessels were undergoing apoptosis. However, in the tumors exposed to the drug combination, the apoptotic cells were in closer association with the blood vessels, and some double-positive apoptotic endothelial cells were observed (Fig. 6*B, arrow*). When caspase-3 was quantified by image analysis (Fig. 6*B*), the combination treatment resulted in a significant increase in apoptotic cells within the tumor.

FTY720, FTY-P (up to 1,000 nmol/L), or PTK/ZK (up to 1,000 nmol/L) failed to induce apoptosis in B16/BL6 cells cultured for 24 or 48 hours in either low serum or in growth medium (Fig. 6*C*; data not shown). Prolonged incubation (>48 hours) of B16 melanoma cells *in vitro* was not possible due to the fast proliferative rate of these cells. None of the compounds exhibited any effect on the proliferation rate of the B16/BL6 cells over 24 hours (Fig. 6*D*). This suggests that these compounds have no apparent effect on the *in vitro* growth of B16/BL6 melanoma cells.

Taken together, the *in vivo* results suggest that B16/BL6 melanoma-bearing mice treated with the combination of FTY720 and PTK/ZK displayed minor effects on the primary tumors but more potent inhibition of the metastatic process, in that metastases were smaller, had a lower blood vessel density, and, as a result thereof, showed increased apoptosis and decreased proliferation of tumor cells.

We also assessed the effect of the immunomodulatory agents on human tumor growth in a nude mouse xenograft model using a well-established MDA-MB-435 human breast carcinoma cell line. The combination of an FTY720 analogue NVP-AAL151 (2.5 mg/kg/d)

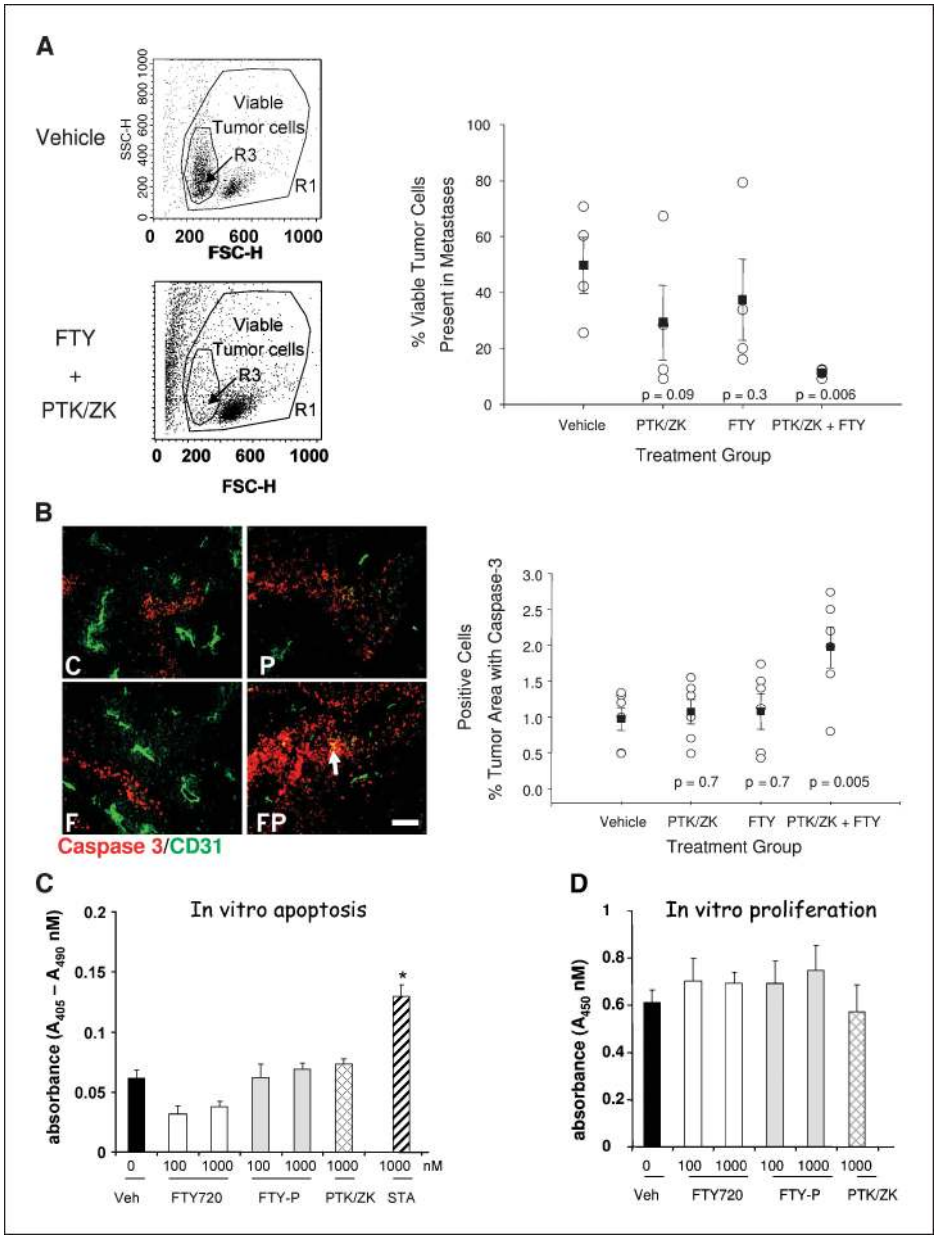

Figure 6. Analysis of viable tumor cells and apoptosis in lymph node metastases. *A,* FACS analysis of viable tumor cells in a metastasis. *Left,* representative scatter plots obtained from a (control) vehicle-treated (*top*) and a (FTY720 + PTK/ZK) combination-treated (*bottom*) disaggregated B16/BL6 metastasis. Tumor cells are detected as a distinct population in the scatter plot and can be accordingly gated (*arrow/R3*). *R1,* gate for all viable cells. *Right,* % living tumor cells in the lymph node metastases as determined by FACS analyses. *Points,* individual (○)/group (■) means; *bars,* SE. Cells (50,000) in R1 were counted from disaggregated tumors; B16/BL6 tumor cells are small and form a distinct population in the scatter plots. *P*s are from one-way ANOVA with post hoc Holm-Sidak tests versus controls. *B,* quantification of apoptosis in the B16 metastases. *Left,* typical immunohistochemically-stained sections for vehicle (*C*), PTK/ZK (*P*), FTY720 (*F*), and a combination of the two drugs (*FP*). Caspase-3, an apoptosis marker (*red*); CD31 (*green*) indicates the blood vessels. *Arrows,* apoptosing vessels in the combination treatment picture (*yellow*). Bar, 100 μm. *Right,* quantification of area of tumor covered by caspase-3-positive apoptosing cells (*red cells*). Six representative fields per tumor section were photographed and quantified. *Points,* individual (○)/group (■) means; *bars,* SE. *P*s are from one-way ANOVA with post hoc Holm-Sidak tests versus controls. *C,* apoptosis of B16/BL6 cells *in vitro*. Cells were incubated with FTY720 or FTY-P (100 and 1,000 nmol/L) or PTK/ZK (1,000 nmol/L) for 24 hours. Staurosporin (1,000 nmol/L) was used as a positive control. The Cell Death kit was used to determine apoptosis. *Columns,* average from triplicate wells; *bars,* SE. *, $P < 0.05$. Representative experiment from three independent experiments. *D,* proliferation of B16/BL6 cells *in vitro*. Cells were incubated with FTY720 or FTY-P (100 and 1,000 nmol/L) or PTK/ZK (1,000 nmol/L) for 24 hours. Proliferation was determined by BrdUrd incorporation. *Columns,* average from triplicate wells (vehicle wells were averaged from 6 wells); *bars,* SE.

with PTK/ZK (100 mg/kg/d) inhibited MDA-MB-435 tumor growth, producing a treated versus control (T/C) of 27%. Whereas the compounds alone produced T/C of 66% and 91%, respectively (data not shown). In further support of this, the inactive analogue NVP-AAL149 in combination with PTK/ZK failed to enhance the antitumor effect (T/C of 96%). These results indicate that combining a VEGFR tyrosine kinase inhibitor with a S1PR modulator can also impair human tumor growth in immunodeficient mice.

Discussion

Our observations confirm the activity of S1P receptor modulators as antiangiogenic agents and extend them to show the novel finding that FTY720, which is phosphorylated to form the active substance FTY-P (10), has antiangiogenic activity in models where either VEGF or S1P are exogenously added as proangiogenic factors. In VEGF-induced angiogenesis models, FTY720 exerted similar extents of inhibition of vascular leakiness, tissue capsule weight, and hemoglobin and Tie-2 content compared with the VEGFR inhibitors used in this study. Additionally, the present study shows for the first time that combination of S1PR modulators and VEGFR inhibitors hold potential for improving antitumor efficacy.

Several studies have clearly defined platelet phospholipids, most notably S1P, as potent angiogenic factors (22). The majority of S1P's actions are mediated by binding to and activating a novel class of receptors belonging to the GPCR family. Of these receptors, $S1P_1$ is the predominant isoform expressed on vascular endothelium. The interaction of S1P with its receptors, most notably $S1P_1$ and $S1P_3$, regulates a number of essential processes in the vascular system, including endothelial cell survival, proliferation, migration, differentiation, and adherens junction assembly (23–25).

$S1P_1$ was shown to be essential for vascular maturation during embryogenesis (26). Down-regulation of $S1P_1$ expression using antisense oligonucleotides or siRNA resulted in the suppression of angiogenesis in a mouse Matrigel plug model and in a mouse tumor model (27, 28). We clearly show that FTY720 pretreatment of HEK293 cells renders them unresponsive to S1P activation, potentially by sequestering the $S1P_1$ internally. Because $S1P_1$ is known to regulate cell survival (e.g., endothelial and mural cells; ref. 29), the FTY720-induced loss of responsiveness to S1P in our chamber model experiments might result in increased apoptosis of the affected cells around the chamber implant, thus contributing to the antiangiogenic effects of the compound. In lymphocytic cells, Matloubian et al. reported that FTY720 treatment down-regulated $S1P_1$ levels, producing lymphocytes unresponsive to S1P exposure (16). It is therefore likely that the antiangiogenic effect of FTY720 in the chamber assay was due to binding to and internalization of $S1P_1$, the major receptor regulating S1P-induced migration of endothelial cells (22) after conversion of FTY720 to its active phosphorylated form.

As FTY-P down-regulates $S1P_1$ receptor in HEK293 cells, and FTY720, FTY-P, and NVP-AAL151 all inhibit S1P-induced calcium mobilization and chemotaxis in human endothelial cells, this suggests that this class of compounds function as receptor antagonists. The differential effects of the FTY720 analogues NVP-AAL151 and NVP-AAL149 (the latter of which can not be phosphorylated) suggest that only FTY720 and NVP-AAL151 may act *in vivo* as acute agonists before inactivating the receptor by internalization. Precisely how FTY-P but not S1P functions to inhibit receptor recycling needs further investigation. Although FTY-P has been shown to have $S1P_1$ agonist activity, our results indicate that its antiangiogenic activity is through $S1P_1$ inactivation/internalization.

Chae et al. showed inhibition of tumor growth and angiogenesis following treatment using a selective $S1P_1$ siRNA (28). These findings along with our observations provide evidence that inactivating $S1P_1$ might lead to inhibition of vascular stabilization, which is thought to be essential for optimal tumor-associated angiogenesis and vasculogenesis. Taken together, the available data indicate that a pure $S1P_1$-selective antagonist may be an effective antiangiogenic agent.

We have shown specificity for abrogation of proangiogenic S1PR signaling by FTY720 and its analogues. In the angiogenesis assays, FTY720 and NVP-AAL151 were active, whereas NVP-AAL149 showed no inhibition in VEGF-driven angiogenesis and only weak inhibition in the S1P-driven angiogenesis model. Although S1P was clearly a less active proangiogenic factor compared with VEGF, when S1P was used to promote angiogenesis, the VEGFR inhibitor NVP-AAL993 had no antiangiogenic activity, whereas the S1P modulators retained inhibitory activity. Although further experimentation is needed, these data suggest that S1P and VEGF promote angiogenesis via different pathways, even if VEGF-promoted angiogenesis apparently involves a process influenced by the S1P pathway (30). In other experiments, we have clearly shown that FTY-P does not affect VEGFR2 expression at the endothelial cell surface, thus eliminating any possibility that FTY-P causes internalization of VEGFR2. Furthermore, we have shown that FTY720 and FTY-P both fail to impede VEGF-induced increases in pMAPK, suggesting that it does not interfere with VEGF binding and signal transduction through VEGFR2.

Using the same FTY720 series of compounds, Sanchez et al. showed selective, potent inhibition of VEGF-induced vascular permeability (10), which is an essential feature for endothelial cell sprouting and migration (1–3). Using a VEGF-dependent permeability assay *in vivo*, we observed potent inhibition of vascular leakiness after FTY720 treatment. This activity of FTY720-inhibiting vascular permeability may be one mechanism of how FTY720 is exerting its antiangiogenic effects. That is, by engaging the S1PRs, FTY-P stimulates the recruitment of endothelial proteins that form adherens junctions, thereby creating a tighter contact between endothelial cells, which may antagonize the effects of VEGF on endothelial permeability (10).

There have been recent reports describing the transactivation of receptor tyrosine kinases by GPCRs and vice versa. Igarashi et al. (30) have shown that treatment of VEGF on vascular endothelial cells specifically induces expression of $S1P_1$ receptors and enhances S1P-mediated signaling pathways. Although there are divergences in signaling pathways evoked by S1P and VEGF (22), it suggests that a functional cross talk is occurring for the regulation of endothelial angiogenic responses. This lead us to test the hypothesis that a potent VEGF receptor inhibitor (PTK/ZK) used in combination with a functional antagonist of the $S1P_1$ receptor might act in concert in inhibiting both tumor angiogenesis as well as tumor growth.

In the syngeneic B16/BL6 melanoma tumor model, monotherapy with either FTY720 or the VEGFR tyrosine kinase inhibitor PTK/ZK alone tended to reduce primary tumor growth, with comparable potency, although the effect of the VEGFR inhibitor reached statistical significance. Similarly, both agents had comparable effects on the size of lymph node metastases as single agents. No convincing combination effects were seen against the primary tumor. However, some potential additional beneficial effects were seen against the lymph node metastases when both compounds were combined. This

is not surprising as the metastatic foci are more likely to be dependent on neovascularization, the primary tumors being in close proximity to the numerous blood vessels already present in the skin. Thus, in the metastasis, by blocking both signaling pathways, a greater antiangiogenic effect was observed, which in turn leads to increased tumor cell apoptosis. The compounds either alone or in combination slowed the tumor growth in this aggressive B16/BL6 model as well as in a well-established xenograft tumor model of breast cancer. There was no overt toxicity observed following treatment of mice using the combination.

We observed that the compounds alone or in combination inhibited metastatic tumor spread and angiogenesis, leading to a decrease in vessel density and tumor cell proliferation and to an enhancement of tumor cell apoptosis. Others have reported that FTY720 can inhibit tumor cell growth *in vitro* and *in vivo* by inducing tumor apoptosis, however, only at very high doses that far exceed those required to induce leukopenia and that would not be tolerable in patients (31). We have observed that B16/BL6 melanoma cells do not express S1PR *in vitro* (data not shown) and that FTY720 did not induce apoptosis of these tumor cells *in vitro*. We were able to show increased apoptosis of tumor cells *in vivo* by FTY720, which suggests that the compound is indirectly affecting tumor cell death by reducing vessel density and thus starving the cells of nutrients.

This tumor is an aggressive melanoma releasing large amounts of VEGF, a factor that recruits many inflammatory cells to the microenvironment. Inflammatory cells, cells that also express S1PR, are thus exposed to the effects of FTY720. Because inflammatory cells can also promote angiogenesis and tumor growth (32), inhibitory effects of FTY720 on these cells may also contribute to its antivascular and antitumor effects.

In conclusion, we show that FTY720, at well-tolerated and clinically relevant doses, significantly attenuated VEGF- and S1P-induced angiogenesis as well as vascular permeability and tumor cell viability. We also show that internalization of $S1P_1$ by FTY-P is a potential mechanism of inhibiting S1P signaling and chemotaxis. These data show that functional antagonism of vascular S1P receptors by FTY720 potently inhibits angiogenesis and, alone or in combination with VEGFR tyrosine kinase inhibition, may provide a novel therapeutic approach for pathologic conditions with dysregulated angiogenesis, such as tumor growth.

Acknowledgments

Received 6/8/2005; revised 9/13/2005; accepted 10/25/2005.

The costs of publication of this article were defrayed in part by the payment of page charges. This article must therefore be hereby marked *advertisement* in accordance with 18 U.S.C. Section 1734 solely to indicate this fact.

We thank Drs. Volker Brinkmann, Peter Lassota, Klaus Seuwen, Georg Martiny Baron, and Danilo Guerini for advice and critically assessing the article and Shobha Thangada, Corinne Manlius, Marina Maurer, and Hans-Peter Muller for their technical assistance.

References

1. Folkman J. Tumor angiogenesis. Adv Cancer Res 1985; 43:175–203.
2. Carmeliet P. Angiogenesis in health and disease. Nat Med 2003;9:653–60.
3. Ferrara N, Gerber HP, LeCouter J. The biology of VEGF and its receptors. Nat Med 2003;9:669–76.
4. Pepper MS. Positive and negative regulation of angiogenesis: from cell biology to the clinic. Vasc Med 1996;1:259–66.
5. English D, Brindley DN, Spiegel S, Garcia JG. Lipid mediators of angiogenesis and the signaling pathways they initiate. Biochim Biophys Acta 2002;1582:228–39.
6. Hla T, Lee MJ, Ancellin N, et al. Sphingosine-1-phosphate: extracellular mediator or intracellular second messenger? Biochem Pharmacol 1999;58:201–7.
7. Tedesco-Silva H, Mourad G, Kahan BD, et al. FTY720, a novel immunomodulator: efficacy and safety results from the first phase 2A study in *de novo* renal transplantation. Transplantation 2004;77:1826–33.
8. Brinkmann V, Davis MD, Heise CE, et al. The immune modulator FTY720 targets sphingosine-1-phosphate receptors. J Biol Chem 2002;277:21453–7.
9. Butler J, Lana D, Round O, LaMontagne K. Functional characterization of sphingosine 1-phosphate receptor agonist in human endothelial cells. Prostaglandins Other Lipid Mediat 2004;73:29–45.
10. Sanchez T, Estrada-Hernandez T, Paik JH, et al. Phosphorylation and action of the immunomodulator FTY720 inhibits vascular endothelial cell growth factor-induced vascular permeability. J Biol Chem 2003;278: 47281–90.
11. Peng X, Hassoun PM, Sammani S, et al. Protective effects of sphingosine 1-phosphate in murine endotoxin-induced inflammatory lung injury. Am J Respir Crit Care Med 2004;169:1245–51.
12. Kenyon B, Voest EE, Chen CC, Flynn E, Folkman J, D'Amato RJ. A model of angiogenesis in the mouse cornea. Invest Ophthalmol Vis Sci 1996;37:1625–32.
13. Wood J, Bold G, Buchdunger E, et al. PTK787/ZK 222584, a novel and potent inhibitor of vascular endothelial growth factor receptor tyrosine kinases, impairs vascular endothelial growth factor-induced responses and tumor growth after oral administration. Cancer Res 2000;60:2178–89.
14. Littlewood-Evans AJ, Mueller U. Stereocilia defects in the sensory hair cells of the inner ear in mice deficient in integrin $\alpha_8\beta_1$. Nat Genet 2000;24:424–8.
15. Liu CH, Thangada S, Lee MJ, Van Brocklyn JR, Spiegel S, Hla T. Ligand-induced trafficking of the sphingosine-1-phosphate receptor EDG-1. Mol Biol Cell 1999;10: 1179–90.
16. Matloubian M, Lo CG, Cinamon G, et al. Lymphocyte egress from thymus and peripheral lymphoid organs is dependent on S1P receptor 1. Nature 2004;427:355–60.
17. Ancellin N, Colmont C, Su J, et al. Extracellular export of sphingosine kinase-1 enzyme. Sphingosine 1-phosphate generation and the induction of angiogenic vascular maturation. J Biol Chem 2002;277:6667–75.
18. Segura BJ, Zhang W, Xiao L, et al. Sphingosine-1-phosphate mediates calcium signaling in guinea pig enteroglial cells. J Surg Res 2004;116:42–54.
19. Cross MJ, Dixelius J, Matsumoto T, Claesson-Welsh L. VEGF-receptor signal transduction. Trends Biochem Sci 2003;28:488–94.
20. Kimura T, Watanabe T, Sato K, et al. Sphingosine 1-phosphate stimulates proliferation and migration of human endothelial cells possibly through the lipid receptors, Edg-1 and Edg-3. Biochem J 2000;348:71–6.
21. Fan D, Liaw A, Denkins YM, et al. Type-1 transforming growth factor-β differentially modulates tumoricidal activity of murine peritoneal macrophages against metastatic variants of the B16 murine melanoma. J Exp Ther Oncol 2002;2:286–97.
22. Liu F, Verin AD, Wang P, et al. Differential regulation of sphingosine-1-phosphate- and VEGF-induced endothelial cell chemotaxis. Involvement of G_{i2}-linked Rho kinase activity. Am J Respir Cell Mol Biol 2001;24:711–9.
23. Paik JH, Chae S, Lee M, Thangada S, Hla T. Sphingosine 1-phosphate induced endothelial cell migration requires the expression of EDG-1 and EDG-3 receptors and Rho dependent activation of $\alpha_v\beta_3$- and β_1-containing integrins. J Biol Chem 2001;276:11830–7.
24. Lee M, Thangada S, Claffey KP, et al. Vascular endothelial cell adherens junction assembly and morphogenesis induced by sphingosine-1-phosphate. Cell 1999;99:301–12.
25. Lee MJ, Thangada S, Paik JH, et al. Akt-mediated phosphorylation of the G protein coupled receptor EDG-1 is required for endothelial cell chemotaxis. Mol Cell 2001;8:693–704.
26. Kono M, Mi Y, Liu Y, et al. S1P1, S1P2 and S1P3 receptors coordinately function during embryonic angiogenesis. J Biol Chem 2004;279:29367–73.
27. Paik JH, Skoura A, Chae SS, et al. Sphingosine 1-phosphate receptor regulation of N-cadherin mediates vascular stabilization. Genes Dev 2004;18:2392–403.
28. Chae SS, Paik JH, Furneaux H, Hla T. Requirement for sphingosine-1-phosphate receptor-1 in tumor angiogenesis demonstrated by *in vivo* RNA interference. J Clin Invest 2004;114:1082–9.
29. Allende ML, Yamashita T, Proia RL. G-protein-coupled receptor $S1P_1$ acts within endothelial cells to regulate vascular maturation. Blood 2003;102:3665–7.
30. Igarashi J, Erwin PA, Dantas AP, Chen H, Michel T. VEGF induces $S1P_1$ receptors in endothelial cells: implications for cross-talk between sphingolipid and growth factor receptors. Proc Natl Acad Sci U S A 2003; 100:10664–9.
31. Azuma H, Horie S, Muto S, et al. Selective cancer cell apoptosis induced by FTY720; evidence for a Bcl-dependent pathway and impairment in ERK activity. Anticancer Res 2003;23:3183–93.
32. Yu JL, Rak JW. Host microenvironment in breast cancer development: inflammatory and immune cells in tumour angiogenesis and arteriogenesis. Breast Cancer Res 2003;5:83–8.